Journal of Civil Engineering, Science and Technology
Volume 12, Issue 1, April 2021

LINEAR AND NONLINEAR FREE VIBRATION ANALYSIS OF RECTANGULAR PLATE

Edward Adah[1*], David Onwuka[2], Owus Ibearugbulem[2] and Chinenye Okere[2]
[1]Department of Civil and Environmental Engineering, University of Calabar, Nigeria.
[2]Department of Civil Engineering, Federal University of Technology Owerri, Nigeria

Date received: 13/07/2020 Date accepted: 31/03/2021
*Corresponding author's email: edwardadah@uncial.edu.ng
DOI: 10.33736/jcest.3338.2021

Abstract — The major assumption of the analysis of plates with large deflection is that the middle surface displacements are not zeros. The determination of the middle surface displacements, u_0 and v_0 along x- and y- axes respectively is the major challenge encountered in large deflection analysis of plate. Getting a closed-form solution to the long standing von Karman large deflection equations derived in 1910 have proven difficult over the years. The present work is aimed at deriving a new general linear and nonlinear free vibration equation for the analysis of thin rectangular plates. An elastic analysis approach is used. The new nonlinear strain displacement equations were substituted into the total potential energy functional equation of free vibration. This equation is minimized to obtain a new general equation for analyzing linear and nonlinear resonating frequencies of rectangular plates. This approach eliminates the use of Airy's stress functions and the difficulties of solving von Karman's large deflection equations. A case study of a plate simply supported all-round (SSSS) is used to demonstrate the applicability of this equation. Both trigonometric and polynomial displacement shape functions were used to obtained specific equations for the SSSS plate. The numerical results for the coefficient of linear and nonlinear resonating frequencies obtained for these boundary conditions were 19.739 and 19.748 for trigonometric and polynomial displacement functions respectively. These values indicated a maximum percentage difference of 0.051% with those in the literature. It is observed that the resonating frequency increases as the ratio of out–of–plane displacement to the thickness of plate (w/t) increases. The conclusion is that this new approach is simple and the derived equation is adequate for predicting the linear and nonlinear resonating frequencies of a thin rectangular plate for various boundary conditions.

***Keywords*:** Membrane strain, total potential energy, linear, nonlinear free vibration, rectangular plates

1.0 INTRODUCTION

Generally, environmental conditions lead a majority of structures as a whole or some parts to be subjected to dynamic loadings during their life span. It is expected most often that, these structures or elements performed optimally with these adverse dynamic circumstances, thereby avoiding the damages caused by the resonating frequencies. Most scholars believe that the maximum amplitude of vibration must be limited for the safety of the structure [1,2,3,4,5]. Of recent, free vibration of plates with large deflection have received considerable attention, because structures of low flexural rigidity are susceptible to large amplitude vibration [6,7,8,9,10,11]. Researchers have analyzed nonlinear vibrations of composite plates because of their lightweight advantage just like thin plates [12,13,14]. The major assumption of the analysis of plates with large deflection is that the middle surface displacements are not zeros [15,16]. Large deflection analysis of rectangular plate anchors mostly on von-Karman type nonlinear strain-displacement relations [16] and are given as equations 1 and 2:

$$\varepsilon_{xx} = \frac{\partial u}{\partial x} = -z\frac{\partial^2 w}{\partial x^2} + \left[\frac{1}{2}\left(\frac{\partial w}{\partial x}\right)^2 + \frac{\partial u_0}{\partial x}\right] \quad (1)$$

$$\varepsilon_{yy} = \frac{\partial v}{\partial y} = -z\frac{\partial^2 w}{\partial y^2} + \left[\frac{1}{2}\left(\frac{\partial w}{\partial y}\right)^2 + \frac{\partial v_0}{\partial y}\right] \quad (2)$$

Where ε_{xx} and ε_{yy} are nonlinear strains along the x- and y-direction respectively; u and v are displacements in x- and y- directions respectively; w is out-of-plane displacement; u0 and v_0 are middle surface displacement in the x- and y- directions respectively.

The first term is bending strain, while the second term in square brackets is the total membrane strain of the plate along the x- or y-direction. The determination of the middle surface displacements, u_0 and v_0 along x- and y- axes respectively is the major challenge encountered in large deflection analysis of plate. Most authors [17,18,19,20,21,22] have assumed expressions for the middle surface displacement rather than determining them from the actual behavior of the plate at the inelastic range. This led to unsatisfactory results beyond the elastic limit of the plate. Also, Airy's stress function is another challenge in the analysis of a plate with large deflection. Unlike earlier authors, some recent authors [23,9,11], determined the stress functions by direct integration. However, their approaches were too complex and full of assumptions that may have construed the actual behavior of a loaded plate. Hence, their results underestimate the carrying capacity of a plate beyond the yield point. Some authors used numerical methods to determine the nonlinear frequencies of a plate by incorporating geometric nonlinearities [24, 25]. This was to avoid the difficulties associated with trying to obtain a closed-form solution to von Karman large deflection equation.

Beyond the yield point, a plate carries the load by the membrane action. The membrane strains are responsible for this additional strength of the plate. Hence, they [26] obtained the nonlinear strain displacement relations as equations 3 and 4:

$$\varepsilon_{xx} = \frac{\partial u}{\partial x} = -z\frac{\partial^2 w}{\partial x^2} + \frac{1}{4}\left(\frac{\partial w}{\partial x}\right)^2 \tag{3}$$

$$\varepsilon_{yy} = \frac{\partial v}{\partial y} = -z\frac{\partial^2 w}{\partial y^2} + \frac{1}{4}\left(\frac{\partial w}{\partial y}\right)^2 \tag{4}$$

The in-plane shear strain, γ_{xy} within x - y plane is given as equation 5:

$$\gamma_{xy} = \frac{\partial u}{\partial y} + \frac{\partial v}{\partial x} = 2\left[-z\frac{\partial^2 w}{\partial x\,\partial y} + \frac{1}{4}\left(\frac{\partial w}{\partial x}\right)\left(\frac{\partial w}{\partial y}\right)\right] \tag{5}$$

And the middle surface strains along the x- and y-axis (ε_{x0} and ε_{y0}) of the plate are given as equations 6 and 7:

$$\varepsilon_{x0} = \frac{\partial u_0}{\partial x} = -\frac{1}{3}\left(\frac{\partial w}{\partial x}\right)^2 \tag{6}$$

$$\varepsilon_{y0} = \frac{\partial u_0}{\partial x} = -\frac{1}{3}\left(\frac{\partial w}{\partial y}\right)^2 \tag{7}$$

In order, to circumvent the use of Airy's stress function and avoid arriving at the same governing equation introduced by von-Karman, this study presents a simple and exact approach to free vibration analysis of rectangular thin plates with large deflection. It is aimed at formulating a general free vibration equation for the analysis of a plate with both small and large deflection for all boundary conditions. This will be achieved via the use of new nonlinear strain displacement equations in the total potential energy functional equation and minimization. It will also, formulate the specific equation for a plate simply supported all-round the edges (SSSS) as a case study.

2.0 MATERIALS AND METHODS

The method used here is the total potential energy/variational method. The formulation is as follows:

2.1 TOTAL POTENTIAL ENERGY FUNCTIONAL

The total potential energy functional, Π, of a thin rectangular plate under free vibration is given as equation 8:

$$\Pi = \frac{1}{2}\int_0^a \int_0^b \int_0^z \left(\sigma_{xx}\,\varepsilon_{xx} + \sigma_{yy}\,\varepsilon_{yy} + \tau_{xy}\gamma_{xy}\right) dxdydz$$

$$-\frac{\rho t\lambda^2}{2}\int_0^a \int_0^b w^2\, dxdy \qquad (8)$$

Where λ Resonating frequency or fundamental natural frequency, t is the plate thickness, ρ is the density of the plate material. And the constitutive relations are given as equation 9:

$$\sigma_x = \frac{E}{1-v^2}\left(\varepsilon_{xx} + v\varepsilon_{yy}\right) \qquad (9a)$$

$$\sigma_y = \frac{E}{1-v^2}\left(\varepsilon_{yy} + v\varepsilon_{xx}\right) \qquad (9b)$$

$$\tau_{xy} = \frac{E(1-v)}{2(1-v^2)}\gamma_{xy} \qquad (9c)$$

Substituting equations 9 into equation 8 yields equation 10:

$$\Pi = \frac{E}{2(1-v^2)}\int_0^a \int_0^b \int_0^z \left[\varepsilon_{xx}{}^2 + 2v\varepsilon_{xx}\,\varepsilon_{yy} + \frac{\gamma_{xy}{}^2}{2} - v\frac{\gamma_{xy}{}^2}{2} + \varepsilon_{yy}{}^2\right] dxdydz$$

$$-\frac{\rho t\lambda^2}{2}\int_0^a \int_0^b w^2\, dxdy \qquad (10)$$

Substituting the nonlinear strain displacement relations in equations 3 and 5 into equation 10, we have equation 11:

$$\Pi = \frac{E}{2(1-\nu^2)}\int_0^a \int_0^b \int_{-t/2}^{t/2} \left\{ z^2\left[\left(\frac{\partial^2 w}{\partial x^2}\right)^2 + 2\left(\frac{\partial^2 w}{\partial x\,\partial y}\right)^2 + \left(\frac{\partial^2 w}{\partial y^2}\right)^2\right]\right.$$

$$-\frac{z}{2}\left[\frac{\partial^2 w}{\partial x^2}.\left(\frac{\partial w}{\partial x}\right)^2 + 2\frac{\partial^2 w}{\partial x\,\partial y}.\left(\frac{\partial w}{\partial x}\right)\left(\frac{\partial w}{\partial y}\right) + \frac{\partial^2 w}{\partial y^2}.\left(\frac{\partial w}{\partial y}\right)^2\right]$$

$$\left.+\frac{1}{16}\left[\left(\frac{\partial w}{\partial x}\right)^4 + 2\left(\frac{\partial w}{\partial y}\right)^2 + \left(\frac{\partial w}{\partial y}\right)^4\right]\right\} dx\,.\,dy\,.\,dz$$

$$-\frac{\rho t\lambda^2}{2}\int_0^a \int_0^b w^2\, dxdy \qquad (11)$$

By carrying out the closed domain integration of equation 11 with respect to z gives equation 12:

$$\Pi$$

$$= \frac{D}{2}\int_0^a \int_0^b \left[\left(\frac{d^2 w}{dx^2}\right)^2 + 2\left(\frac{d^2 w}{dxdy}\right)^2 + \left(\frac{d^2 w}{dy^2}\right)^2\right] dxdy$$

$$+\frac{gD}{2\times 16}\int_0^a \int_0^b \left(\left[\frac{\partial w}{\partial x}\right]^4 + 2\left[\frac{\partial w}{\partial x}\right]^2\left[\frac{\partial w}{\partial y}\right]^2 + \left[\frac{\partial w}{\partial y}\right]^4\right) dxdy$$

$$-\frac{\rho t\lambda^2}{2}\int_0^a \int_0^b w^2\, dxdy \qquad (12)$$

Where: $D = \frac{Et^3}{12(1-\nu^2)}$; $g = \frac{12}{t^2}$; $gD = \frac{12}{t^2}\times\frac{Et^3}{12(1-\nu^2)}$

$$= \frac{Et}{(1-\nu^2)} \qquad (13a-c)$$

Writing equation 12 in terms of the non-dimensional coordinates, R = x/a and Q = y/b, for 0≤R≤1; 0≤Q≤1, we have equation 14:

$$\Pi = \frac{bD}{2a^3}\int_0^1\int_0^1\left[\left(\frac{d^2w}{dR^2}\right)^2 + \frac{2}{\mathcal{2}^2}\left(\frac{d^2w}{dRdQ}\right)^2 + \frac{1}{\mathcal{2}^4}\left(\frac{d^2w}{dQ^2}\right)^2\right]dxdy$$
$$+ \frac{bgD}{2a^3\times 16}\int_0^1\int_0^1\left[\left(\frac{\partial w}{\partial R}\right)^4 + \frac{2}{\mathcal{2}^2}\left(\frac{\partial w}{\partial R}\right)^2\left(\frac{\partial w}{\partial Q}\right)^2 + \frac{1}{\mathcal{2}^4}\left(\frac{\partial w}{\partial Q}\right)^4\right]dxdy$$
$$- \frac{ab\rho t\lambda^2}{2}\int_0^1\int_0^1 w^2\,dRdQ \qquad (14)$$

To minimizing equation 12 with respect to w, u_0 and v_0, let rewrite equation 12 as equation 15:

$$\Pi = \frac{D}{2}\int_0^a\int_0^b\left[\frac{d^3}{dx^3}\frac{dw^2}{dx} + \frac{d^3}{dxdy^2}\frac{dw^2}{dx} + \frac{d^3}{dx^2dy}\frac{dw^2}{dy} + \frac{d^3}{dy^3}\frac{dw^2}{dy}\right]dxdy$$
$$+ \frac{gD}{2\times 16}\int_0^a\int_0^b\left[\frac{\partial^2}{\partial x^2}\left(\frac{\partial w^2}{\partial x}\right)^2 + \frac{\partial}{\partial x}.\frac{\partial}{\partial x}.\frac{\partial}{\partial y}.\frac{\partial}{\partial y}\,(w^2)^2\right.$$
$$\left. + \frac{\partial^2}{\partial y^2}\left(\frac{\partial w^2}{\partial y}\right)^2\right]dxdy - -\frac{\rho t\lambda^2}{2}\int_0^a\int_0^b w^2\,dxdy \qquad (15)$$

Note that minimization with respect to u_0 and v_0 shall be based on the differential part without involving the constants coefficients.

Now, minimizing equation 15 with respect to w gives equation 16a:

$$\frac{\partial\Pi}{\partial w} = \int_0^a\int_0^b\{D\left[\frac{\partial^4 w}{\partial x^4} + 2\frac{\partial^4 w}{\partial x^2\partial y^2} + \frac{\partial^4 w}{\partial y^4}\right] + \frac{gD}{16}\left[\left(\frac{\partial w}{\partial x}\right)^2\frac{\partial^2 w}{\partial x^2} + \left(\frac{\partial w}{\partial y}\right)^2\frac{\partial^2 w}{\partial x^2} + \left(\frac{\partial w}{\partial x}\right)^2\frac{\partial^2 w}{\partial y^2}\right.$$
$$\left. + \left(\frac{\partial w}{\partial y}\right)^2\frac{\partial^2 w}{\partial y^2}\right] - \rho t\lambda^2 w\}dxdy = 0$$

For this equation to be true, the integrand must be equal to zero.

$$D\left[\frac{\partial^4 w}{\partial x^4} + 2\frac{\partial^4 w}{\partial x^2\partial y^2} + \frac{\partial^4 w}{\partial y^4}\right]$$
$$+ \frac{gD}{16}\left[\left(\frac{\partial w}{\partial x}\right)^2\frac{\partial^2 w}{\partial x^2} + \left(\frac{\partial w}{\partial y}\right)^2\frac{\partial^2 w}{\partial x^2} + \left(\frac{\partial w}{\partial x}\right)^2\frac{\partial^2 w}{\partial y^2} + \left(\frac{\partial w}{\partial y}\right)^2\frac{\partial^2 w}{\partial y^2}\right]$$
$$- \rho t\lambda^2 w = 0 \qquad (16a)$$

Minimizing equation 15 with respect to (dw^2/dx) gives equation 16b:

$$\frac{\partial\Pi}{\partial\left(\frac{\partial w^2}{\partial x}\right)} = \frac{D}{2}\frac{\partial}{\partial x}\left[\frac{d^2}{dx^2} + \frac{d^2}{dy^2}\right] + gDc_2^2\frac{\partial}{\partial x}\left[\left(\frac{\partial w}{\partial x}\right)^2 + \left(\frac{\partial w}{\partial y}\right)^2\right] - 0 = 0$$

That is:

$$\frac{\partial\Pi}{\partial\left(\frac{\partial w^2}{\partial x}\right)} = \frac{gD}{16}.\frac{\partial}{\partial x}\left[\left(\frac{\partial w}{\partial x}\right)^2 + \left(\frac{\partial w}{\partial y}\right)^2\right] = 0$$

That is:

$$\left[\left(\frac{\partial w}{\partial x}\right)^2 + \left(\frac{\partial w}{\partial y}\right)^2\right] = 0 \qquad (16b)$$

Minimizing equation 15 with respect to (dw^2/dy) gives equation 16c:

$$\frac{\partial \Pi}{\partial\left(\frac{\partial w^2}{\partial y}\right)} = \frac{D}{2}\frac{\partial}{\partial y}\left[\frac{d^2}{dx^2}+\frac{d^2}{dy^2}\right]+\frac{gD}{16}\frac{\partial}{\partial y}\left[\left(\frac{\partial w}{\partial x}\right)^2+\left(\frac{\partial w}{\partial y}\right)^2\right]-0=0$$

That is:

$$\frac{\partial \Pi}{\partial\left(\frac{\partial w^2}{\partial y}\right)} = \frac{gD}{16}\cdot\frac{\partial}{\partial y}\left[\left(\frac{\partial w}{\partial x}\right)^2+\left(\frac{\partial w}{\partial y}\right)^2\right]=0$$

That is:

$$\left[\left(\frac{\partial w}{\partial x}\right)^2+\left(\frac{\partial w}{\partial y}\right)^2\right]=0 \qquad (16c)$$

Equation 16a is the governing equation, while equations 16b and 16c are the displacement compatibility equations.

It is seen from equations 16b and 16c that;

$$\left(\frac{\partial w}{\partial x}\right)^2=-\left(\frac{\partial w}{\partial y}\right)^2 \qquad (17)$$

Substituting equation 17 into equation 6 we have equation 18:

$$\varepsilon_{x0}=\frac{\partial u_0}{\partial x}=\frac{1}{3}\left(\frac{\partial w}{\partial y}\right)^2 \qquad (18)$$

Comparing equations 7 and 18 we have equation 19:

$$\varepsilon_{x0}=-\varepsilon_{y0} \qquad (19)$$

Substituting equation 17 into equation 16a we have equation 20:

$$D\left[\frac{\partial^4 w}{\partial x^4}+2\frac{\partial^4 w}{\partial x^2\partial y^2}+\frac{\partial^4 w}{\partial y^4}\right]-\rho t\lambda^2 w=0 \qquad (20)$$

Let the solution of equation 20 be in the form of equation 21:

$$w=a_i h_x \times b_i h_y = Ah \qquad (21)$$

Substituting equation 21 into equation 14 gives equation 22:

$$\Pi = \frac{bDA^2}{2a^3}\int_0^1\int_0^1\left[\left(\frac{\partial^2 h}{\partial R^2}\right)^2+\frac{2}{\mathcal{2}^2}\left(\frac{\partial^2 h}{\partial R\partial Q}\right)^2+\frac{1}{\mathcal{2}^4}\left(\frac{\partial^2 h}{\partial Q^2}\right)^2\right]dRdQ$$
$$+\frac{bgDA^4}{2a^3*16}\int_0^1\int_0^1\left[\left(\frac{\partial h}{\partial R}\right)^4+\frac{2}{\mathcal{2}^2}\left(\frac{\partial h}{\partial R}\right)^2\left(\frac{\partial h}{\partial Q}\right)^2+\frac{1}{\mathcal{2}^4}\left(\frac{\partial h}{\partial Q}\right)^4\right]dRdQ$$
$$-\frac{ab\rho t\lambda^2A^2}{2}\int_0^1\int_0^1 h^2\,dRdQ \qquad (22)$$

Where A is the amplitude of deflection, and h is the displacement shape profile.

Minimizing equation 22 with respect to A gives equation 23:

$$\frac{\partial \Pi}{\partial A}=\frac{AbD}{a^3}\iint\left[\left(\frac{d^2h}{dR^2}\right)^2+\frac{2}{\mathcal{2}^2}\left(\frac{d^2h}{dRdQ}\right)^2+\frac{1}{\mathcal{2}^4}\left(\frac{d^2h}{dQ^2}\right)^2\right]dR\,dQ+\frac{A^3bgD}{8a^3}\iint\left[\left(\frac{\partial h}{\partial R}\right)^4+\frac{2}{\mathcal{2}^2}\left(\frac{\partial h}{\partial R}\right)^2\left(\frac{\partial h}{\partial Q}\right)^2+$$
$$\frac{1}{\mathcal{2}^4}\left(\frac{\partial h}{\partial Q}\right)^4\right]dR\,dQ-ab\rho t\lambda^2A\int_0^1\int_0^1 h^2\,dRdQ=0 \qquad (23)$$

Multiply equation 23 by $\frac{a^3}{Db}$, we have equation 24:

$$\int_0^1\int_0^1\left[\left(\frac{\partial^2 h}{\partial R^2}\right)^2+\frac{2}{\mathcal{2}^2}\left(\frac{\partial^2 h}{\partial R\partial Q}\right)^2+\frac{1}{\mathcal{2}^4}\left(\frac{\partial^2 h}{\partial Q^2}\right)^2\right]dRdQ$$

$$+\ \frac{gA^2}{8}\int_0^1\int_0^1\left[\left(\frac{\partial h}{\partial R}\right)^4+\frac{2}{\mathcal{2}^2}\left(\frac{\partial h}{\partial R}\right)^2\left(\frac{\partial h}{\partial Q}\right)^2\ +\frac{1}{\mathcal{2}^4}\left(\frac{\partial h}{\partial Q}\right)^4\right]dRdQ$$

$$-\frac{\rho t\lambda^2 a^4}{D}\int_0^1\int_0^1 h^2\,dRdQ\ =0 \qquad (24)$$

Rewriting equation 24 in symbolic form, we have equation 25:

$$\left[k_{bx}+\frac{2k_{bxy}}{\mathcal{2}^2}+\frac{k_{by}}{\mathcal{2}^4}\right]+\frac{gA^2}{8}\left[k_{mx}+\frac{2k_{mxy}}{\mathcal{2}^2}+\frac{k_{my}}{\mathcal{2}^4}\right]=\rho t\lambda^2\frac{a^4}{D}k_\lambda \qquad (25)$$

$$Where, k_{bx}=\int_0^1\int_0^1\left(\frac{\partial^2 h}{\partial R^2}\right)^2 dRdQ;\qquad k_{bxy}=\int_0^1\int_0^1\left(\frac{\partial^2 h}{\partial R\partial Q}\right)^2 dRdQ$$

$$k_{by}=\int_0^1\int_0^1\left(\frac{\partial^2 h}{\partial Q^2}\right)^2 dRdQ;\qquad k_{mx}=\int_0^1\int_0^1\left(\frac{\partial h}{\partial R}\right)^4 dRdQ$$

$$k_{mxy}=\int_0^1\int_0^1\left(\frac{\partial h}{\partial R}\right)^2\left(\frac{\partial h}{\partial Q}\right)^2 dRdQ;\qquad k_{my}=\int_0^1\int_0^1\left(\frac{\partial h}{\partial Q}\right)^4 dRdQ$$

$$k_\lambda=\int_0^1\int_0^1 h^2\,dRdQ \qquad (26a-f)$$

Subscripts b and m denote bending and membrane parts respectively.

From equation 25, we have equation 27:

$$K_{bT}+\frac{gA^2}{8}K_{mT}=\rho t\lambda^2\frac{a^4}{D}k_\lambda \qquad (27)$$

$$Where, K_{bT}=\left[k_{bx}+\frac{2k_{bxy}}{\mathcal{2}^2}+\frac{k_{by}}{\mathcal{2}^4}\right];\ K_{mT}=\left[k_{mx}+\frac{2k_{mxy}}{\mathcal{2}^2}+\frac{k_{my}}{\mathcal{2}^4}\right] \qquad (28)$$

K_{bT} is the total bending stiffness and K_{mT} is the total membrane stiffness.

Substitute equations 11a and 11b into equation 27 we have equation 29:

$$\frac{\rho\lambda^2 a^4}{Et^2}=\frac{1}{12(1-v^2)}\left[\frac{K_{bT}}{k_\lambda}+\frac{3}{2}\frac{K_{mT}}{k_\lambda}\left(\frac{A}{t}\right)^2\right] \qquad (29)$$

From equation 29, the linear/nonlinear resonating frequency is given as equation 30:

$$\lambda=\sqrt{\left[\frac{K_{bT}}{k_\lambda}+\frac{3}{2}\frac{K_{mT}}{k_\lambda}\left(\frac{A}{t}\right)^2\right]}*\frac{1}{a^2}\sqrt{\frac{D}{\rho t}} \qquad (30)$$

Where $\lambda=\lambda_x$ is the linear/nonlinear resonating frequency along the x-axis. Equation 30 is the general linear/nonlinear resonating frequency of a rectangular isotropic plate undergoing free vibration. Also from equation 27, the ratio of the amplitude of deflection to the thickness of the plate can be given as

$$\left(\frac{A}{t}\right)^2 = 8(1-v^2) * \frac{k_\lambda}{K_{mT}} * \frac{\rho\lambda^2 a^4}{Et^2} - \frac{2}{3}\frac{K_{bT}}{K_{mT}} \tag{31}$$

And the maximum displacement, w, at the corresponding resonating frequency is as equation 32:

$$w = \sqrt{\frac{2}{3}\frac{(h_{\max})^2}{K_{mT}}\left[\frac{12(1-v^2)k_\lambda\, a^2\rho{\lambda_x}^2}{E} - t^2 K_{bT}\right]} \tag{32}$$

2.2 NUMERICAL APPLICATION

Let's consider a simply supported rectangular plate (SSSS), the trigonometric displacement shape profile, h, is given as equation 33:

$$h = (Sin\,\pi R)\,(Sin\,\pi Q);\quad h_x = (Sin\,\pi R)\,;\ h_y = (Sin\,\pi Q) \tag{33}$$

While the polynomial displacement shape profile is given as equation 34:

$$h = (\mathrm{R} - 2\mathrm{R}^3 + \mathrm{R}^4)(\mathrm{Q} - 2\mathrm{Q}^3 + \mathrm{Q}^4) \tag{34a}$$

$$Where, \mathrm{h}_x = (\mathrm{R} - 2\mathrm{R}^3 + \mathrm{R}^4);\ \mathrm{h}_y = (\mathrm{Q} - 2\mathrm{Q}^3 + \mathrm{Q}^4) \tag{34b}$$

Evaluating the plate stiffness from equations 26a-f using the trigonometric displacement shape profile, we have the results obtained presented in row 2 of Table 1. While stiffness results obtained from polynomial displacement shape profile are presented in row 3 of Table 1.
Substituting these stiffness values in equation 30 we have the specific equation for linear/nonlinear resonating frequency for SSSS plate undergoing free vibration, as presented in Table 2.

3.0 RESULTS AND DISCUSSION

Table 1 showed the plate stiffness results obtained from equations 26a-f using both trigonometric and polynomial displacement profiles. While Table 2 showed the various new equations developed from this present work.

Table 1 Stiffness values for SSSS plate from both Trigonometric and Polynomial Analyses

Ks	$\mathbf{k_{bx}}$	$\mathbf{k_{bxy}}$	$\mathbf{k_{by}}$	$\mathbf{k_{mx}}$	$\mathbf{k_{mxy}}$	$\mathbf{k_{my}}$	$\mathbf{k_{Nx}}$
Trig.	$\frac{\pi^4}{4}$	$\frac{\pi^4}{4}$	$\frac{\pi^4}{4}$	$\frac{9\pi^4}{64}$	$\frac{\pi^4}{64}$	$\frac{9\pi^4}{64}$	$\frac{\pi^2}{2}$
Poly.	0.236190	0.235918	0.236190	0.001300	0.000138	0.001300	0.002421

The new mathematical models formulated are presented in Table 2. These equations will help in the easy prediction of the frequency of a loaded plate at a particular deflection based on the thickness of the plate. The three parameters unknown in the equation are the frequency, λ_{Max}, the deflection or displacement, w, and the plate thickness, t. In designing, knowing the limiting or maximum deflection of a plate, and the maximum frequency required to avoid resonance, a designer can comfortable with this equation determine the plate thickness required to avoid failure. Any of the parameters can be determine by knowing the values of the other parameters. Also, when the deflection, w, is zero, the equation will predict the fundamental natural frequency of the plate. That means, the plate deflection is still within the elastic limit and still linear. The use of both the polynomial and trigonometric shape functions in the formulation of the specific equation for the SSSS boundary condition provided an easy alternative to analysts and indicate the adequacy of the new approach. The numerical results obtained from equations 29 and 30 (shown in Table 2) are presented in columns 2 and 3 for linear/nonlinear resonating frequency parameter and in columns 6 and 7 for linear and nonlinear resonating frequency of plate in Table 3.

Table 2 New Linear/Nonlinear Resonating Frequency Equations from this work

SN	Description	Equation
1	General Linear/Nonlinear Resonating Frequency Parameter, $\frac{\rho\lambda^2 a^4}{Et^2}$	$\frac{\rho\lambda^2 a^4}{Et^2} = \frac{1}{12(1-v^2)}\left[\frac{K_{bT}}{k_\lambda} + \frac{3}{2}\frac{K_{mT}}{k_\lambda}\frac{1}{(h_{\max})^2}\left(\frac{w}{t}\right)^2\right]$
2	General Linear/Nonlinear Resonating Frequency, λ	$\lambda_{Max} = \sqrt{\left[\frac{K_{bT}}{k_\lambda} + \frac{3}{2}\frac{K_{mT}}{k_\lambda}\frac{1}{(h_{\max})^2}\left(\frac{w}{t}\right)^2\right]} * \frac{1}{a^2}\sqrt{\frac{D}{\rho t}}$
3	Dynamic Amplitude of Displacement to plate thickness, $\left(\frac{A}{t}\right)^2$	$\left(\frac{A}{t}\right)^2 = 8(1-v^2) * \frac{k_\lambda}{K_{mT}} * \frac{\rho\lambda^2 a^4}{Et^2} - \frac{2}{3}\frac{K_{bT}}{K_{mT}}$
4	General Plate Displacement Equation at point of Maximum displacement, w	$w = \sqrt{\frac{2}{3}\frac{(h_{\max})^2}{K_{mT}}\left[\frac{12(1-v^2)k_\lambda\, a^2\rho{\lambda_x}^2}{E} - t^2 K_{bT}\right]}$
5	Linear/Nonlinear Resonating Equation for SSSS Plate at point of maximum displacement (Trigonometric), λ_{Max}	$\lambda_{Max} = \frac{1}{a^2 2^2}\Big[\{97.4090910849(2^4+1) + 194.81818216982^2\} + \{82.1889206029(2^4+1) + 18.264204578422^2\}\left(\frac{w}{t}\right)^2\Big]^{\frac{1}{2}}\sqrt{\frac{D}{\rho t}}$
6	Linear/Nonlinear Resonating Equation for SSSS Plate at point of maximum displacement (Polynomial), λ_{Max}	$\lambda_{Max} = \frac{1}{a^2 2^2}\Big[\{97.5483870968(2^4+1) + 194.872008324722^2\} + \{84.4335749229(2^4+1) + 17.952197836822^2\}\left(\frac{w}{t}\right)^2\Big]^{\frac{1}{2}}\sqrt{\frac{D}{\rho t}}$

To validate the results obtained from this work, both trigonometric and polynomial displacement shape functions were used in the analysis. These numerical results were compared in columns 4 and 8 of Table 3 for frequency parameter and linear/nonlinear resonating frequency respectively. The percentage differences for the frequency parameter had a maximum value of 1.537 while those of resonating frequencies were less than 1. This is negligible and showed a good agreement between the results of the two numerical approaches. Also, there is a good agreement between the critical resonating frequencies (that is, the fundamental frequencies) between this work and those in literature as shown in Table 4. The fundamental frequencies obtained from the use of trigonometric and polynomial displacement shape profiles indicated a percentage difference of -0.043, meaning that, the trigonometric displacement shape profile yield results which are lower bound to those obtain by polynomial displacement shape profile. However, the present fundamental frequency value is the same as the value obtained by Leissa & Quta (2011) and Deutsch et al. (2019). It indicates that the new equations developed by this work were adequate for free vibration analysis of rectangular plates. These results also indicated that the nonlinear frequency increases as the w/t increase. In contrast to Figure 1, the nonlinear frequency decreases as the aspect ratio (b/a) increase. This is in the agreement with the work of Onodagu (2018) and reflects the behavior of thin rectangular plates. However, Figure 1 showed a complete agreement between the results of the two displacement shape profiles. Besides, the gradual increase in the nonlinear frequency from the fundamental frequency as w/t increases indicated the adequacy of the results. This indicates the actual behavior of the SSSS rectangular plate before ultimate failure. It's also indicated that the SSSS plate does not fail geometrically but may fail materially.

Table 3 Linear/Nonlinear Resonating Frequency Parameter values and Linear/Nonlinear Resonating Frequency, for Aspect Ratio, $\mathcal{Z} = 1$

$\frac{w}{t}$	$\frac{\rho\lambda^2 a^4}{Et^2}$	% Difference $100(F_1-F_2)/F_1$		$\lambda_{Max} = \frac{f}{a^2} * \sqrt{\frac{D}{\rho t}}$ $= \sqrt{\left[\frac{K_{bT}}{k_\lambda} + \frac{3}{2}\frac{K_{mT}}{k_\lambda}\frac{1}{(h_{max})^2}\left(\frac{w}{t}\right)^2\right]}$		%Difference $100(f_1-f_2)/f_1$
Col. 1	**Col. 2**	**Col.3**	**Col.4**	**Col.5**	**Col.6**	**Col. 7**	**Col. 8**
	Trig. F_1	**Poly. F_2**			**Trig. f_1**	**Poly. f_2**	
0	35.681	35.711	-0.085		19.739	19.748	-0.043
0.25	36.146	36.187	-0.114		19.867	19.879	-0.057
0.5	37.539	37.613	-0.196		20.247	20.267	-0.098
0.75	39.862	39.989	-0.319		20.864	20.897	-0.159
1	43.115	43.317	-0.469		21.698	21.749	-0.234
1.25	47.296	47.595	-0.632		22.726	22.798	-0.315
1.5	52.406	52.823	-0.796		23.922	24.017	-0.397
1.75	58.446	59.003	-0.952		25.263	25.383	-0.475
2	65.415	66.133	-1.097		26.727	26.873	-0.547
2.25	73.313	74.213	-1.228		28.295	28.468	-0.612
2.5	82.141	83.245	-1.344		29.950	30.150	-0.670
2.75	91.897	93.227	-1.447		31.678	31.907	-0.721
3	102.583	104.159	-1.537		33.469	33.726	-0.766

Table 4 Comparison Fundamental frequency from this work with those in literature

Present work, Trig.	**Present work, Poly**	**Leissa & Quta. (2011); Deutsch, *et al* (2019) [27]**	**Onodagu (2018)**	**Njoku, (2018)**
19.739	19.748	19.739	19.748	19.749
%Difference	-0.043	0.000	-0.0456	-0.05064

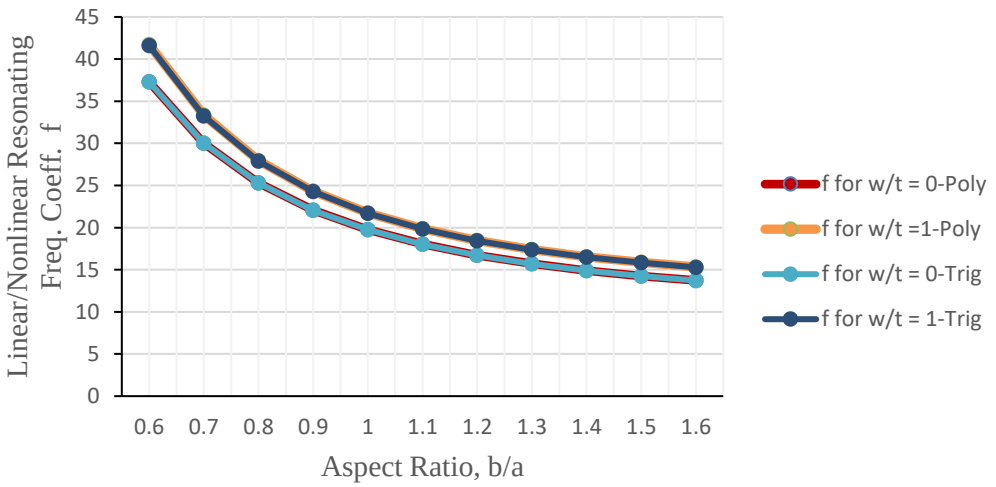

Figure 1 Relationship between Linear/Nonlinear Resonating Frequency and the Aspect Ratio (b/a) for given Displacement to thickness ratio (w/t).

This means that the failure of the plate based on these results may be due mostly to material imperfection such as manufacturing defects, use of substandard materials, etc rather than failure due to the shape of the plate or support conditions used. Since there is a continuous increase in the frequency beyond the fundamental frequency as w/t increases. This is in agreement with the works of Oguaghamba (2015) and Onoduga (2018). Furthermore, it's showed that both displacement shape profiles were adequate for rectangular plate analysis for both small and large deflection.

4.0 CONCLUSION

The present work had derived a new general linear/nonlinear free vibration equation for the analysis of rectangular thin plates. It's had also, derived the linear/nonlinear free vibration equations for SSSS rectangular plate by using both trigonometric and polynomial analyses. The approach used here is independent of the complex von Karman nonlinear equations of large deflection and Airy's functions. The results obtained for the linear and nonlinear frequencies using polynomial and trigonometric shape functions had agreed very closely with each other and with those in literature with percentage difference less than 1. Also, the results indicated that the nonlinear frequency increases as the w/t increase but decrease with increase in aspect ratio. Furthermore, it was observed that the SSSS plate will not fail geometrically but rather it may fail materially. This means that the failure of the plate based on these results may be due mostly to material imperfection such as manufacturing defects, use of substandard materials, etc rather than failure due to the shape of the plate or support conditions used. This is in agreement with the works of Oguaghamba (2015) and Onoduga (2018). It is concluded that this approach is simpler and exact and has eliminated greatly the difficulties associated with closed-form large deflection analysis of rectangular plates. Also, that the developed equations are adequate for linear/nonlinear free vibration analysis of rectangular plate.

Conflict of Interests

The authors declare that there is no conflict of interests regarding the publication of this paper.

Acknowledgement

The authors wish to acknowledge the management of the University of Calabar and Federal University of Technology Owerri, for supporting this work by creating enabling environment for us to carry out this research work.

References

[1] Leissa , A. W. & Quta, M. S. (2011). Vibration of Continuous Systems. McGraw-Hill Company, USA.

[2] Dash, A. K. (2010). Large Amplitude Free Vibration Analysis of Composite Plates by Finite Element Method. M.Sc Thesis, National Institute of Technology, Rourkela.

[3] Ducceschi, M. (2014). Nonlinear Vibrations of Thin Rectangular Plates: A Numerical Investigations with Application to Wave Turbulence and Sound Synthesis. Vibrations (Physics.class-ph).ENSTA Panotech,

[4] Ibearugbulem, O. M, Ezeh, J. C. & Ettu, L. O. (2014). Energy Methods in Theory of Rectangular Plates: Use of Polynomial Shape Functions. Liu House of Excellence Ventures, Owerri.

[5] Adah, E. I., Ibearugbulem, O. M., Onwuka, D. O. & Okoroafor, S. U. (2019). Determination of Resonating Frequency of Thin Rectangular Flat Plates. International Journal of Civil and Structural Engineering Research, **7** (1), 16-22, www.researchpublish.com.

[6] Hashemi, S. & Jaberzadeh, E. (2012). A Finite Strip Formulation for Nonlinear Free Vibration of Plates, *15 WCEE*, Lisboa.

[7] Kumar, R. & Goytom, D. (2017). Postbuckling and Nonlinear Free Vibration Response of Elastically Supported Laminated Composite Plates with Uncertain System Properties in Thermal Environment. Frontiers in Aerospace Engineering, **6** (): 1-27.

[8] Varzandian, G. A. & Ziaei, S. (2017). Analytical Solution of Nonlinear Free Vibration of Thin Rectangular Plates with Various Boundary Conditions based on Non-local Theory. Amir Kabir Journal of science and research mechanical engineering, **48** (4): 121-124.

[9] Onodagu, P. D. (2018). Nonlinear Dynamic Analysis of Thin Rectangular Plates using Ritz Method. PhD Thesis, Federal University of Technology, Owerri, Nigeria.

[10] Yosibash, Z. & Kirby, R. M. (2005). Dynamic Response of various von-Karman nonlinear plate models and their 3-D counterparts. International Journal of Solids & Structures, 42, 2517-2531. DOI: 10.1016/j.ijolstr.2004.10.006

[11] Mattieu, G., Tyekolo, D. & Belay, S. (2017). The nonlinear bending of simply supported elastic plate. RUDN Journal of Engineering researches. 18 (1), 58-69. DOI: 10.22363/2312-8143-2017-18-1-58-69.
[12] Kucukrendeci, I. (2017). Nonlinear vibration analysis of composite plates on elastic foundations in thermal environments. AKU. J. Sci. Eng. 17, 790-796. DOI: 10.5578(fmbd.57619).
[13] Zergoune, Z., Harras, B. & Benanar, R. (2015). Nonlinear Free Vibration vibration of C-C-SS-SS symmetrically laminated carbon fibre reinforced plastic (CFRP) rectangular composite plates. World Journal of mechanics. 5, 22-32, DOI: 10.4236/wjm.2015.52003
[14] El Kaak, R. & Bikri, K (2016). Geometrically Nonlinear Free Axisymmetric Vibrations Analysis of thin circular functionally graded plates using iterative and explicit analysis solution. International Journal of Acoustics and Vibration, 21(2), 209-221. DOI: 10.20855/ijar.2016.21.2414.
[15] Levy, S. (1942). Bending of Rectangular Plates with Large Deflections. Technical notes: National Advisory Committee for Aeronautics (NACA), N0. 846.
[16] Enem, J. I. (2018). Geometrically Nonlinear Analysis of Isotropic Rectangular Thin Plates Using Ritz Method. PhD Thesis, Federal University of Technology, Owerri, Nigeria.
[17] Elsami, M. R. (2018). Buckling and Postbuckling of Beams, Plates, and Shells. Springer International Publishing AG.
[18] Manuel, S. (1984). Analytical Results for Postbuckling Behavior of Plates in Compression and in Shear. National Aeronautics and Space Administration (NASA). NASA Technical Memorandum 85766.
[19] Bloom, F. & Coffin, D. (2001). Thin Plate Buckling and Postbuckling. London: Chapman & Hall/CRC.
[20] Byklum, E. & Amdahl, J. (2002). A Simplified Method for Elastic Large Deflection Analysis of Plates and Stiffened Panels due to Local Buckling. Thin-Walled Structures, **40** (): 925–953.
[21] Tanriöver H. & Senocak, E. (2004). Large Deflection Analysis of Unsymmetrically Laminated Composite plates: Analytical–numerical type Approach. International Journal of Non-linear Mechanics, **39**: 1385–1392.
[22] GhannadPour, S. A. M. & Alinia, M. M. (2006). Large Deflection Behavior of Functionally Graded Plates under Pressure Loads. Composite Structures**, 75**: 67–71.
[23] Shufrin, I., Rabinovitch, O. & Eisenberger, M. (2008). A Semi-analytical Approach for the Nonlinear Large Deflection Analysis of Laminated Rectangular Plates under General out-of-plane loading. International Journal of Non-Linear Mechanics, **43**:328–340.
[24] Ducceschi, M., Touze, C., Bilbao, S. & Webb, C. J. (2013). Nonlinear dynamics of rectangular plates: investigation of model interaction in free and forced vibrations. Acta Mech, DOI: 10.1007/s00707-013-0931-1.
[25] Stoykov, S. & Margenov, S. (2016). Finite Element Method for Nonlinear Vibration Analysis of Plates. Springer International Publishing Switzerland, 17-27. DOI: 10.1007/978-3-319-32207-0_2
[26] Ibearugbulem, O. M., Adah, E. I., Onwuka, D. O. & Okere, C. E. (2020). Simple and Exact Approach to Postbuckling Analysis of Rectangular Plate, SSRG International Journal of Civil Engineering, **7** (6): 54-64, www.internationaljournalssrg.org.
[27] Deutsch, A., Tenenbaum, J., & Eisenberger, M. (2019). Benchmark Vibration Frequencies of Square Thin Plates with all Possible Combinations of Classical Boundary Conditions. International Journal of Structural Stability and Dynamics, 19(11), 1950131-1-1950131-16, DOI: 10.1142/S0219455419501311